Journal of
Synchrotron Radiation

ISSN 0909-0495

Received 9 December 2008
Accepted 1 April 2009

First observation of natural circular dichroism spectra in the extreme ultraviolet region using a polarizing undulator-based optical system and its polarization characteristics

Masahito Tanaka,[a]* Kazutoshi Yagi-Watanabe,[a] Fusae Kaneko[a] and Kazumichi Nakagawa[b]

[a]Research Institute of Instrumentation Frontier, National Institute of Advanced Industrial Science and Technology (AIST), Central 2, Umezono 1-1-1, Tsukuba, Ibaraki 305-8568, Japan, and [b]Graduate School of Human Development and Environment, Kobe University, Tsurukabuto 3-11, Nada-ku, Kobe 657-8501, Japan. E-mail: masahito-tanaka@aist.go.jp

Natural circular dichroism (CD) spectra in the extreme ultraviolet (EUV) region down to a wavelength of 80 nm have been observed for the first time, using an alanine thin film deposited on sodium salicylate coated glass as a sample. Calibrated EUV-CD spectra of L-alanine exhibited a large negative peak at around 120 nm and a positive CD signal below 90 nm, which were roughly predicted by theoretical calculations. A CD measurement system with an Onuki-type polarizing undulator was used to obtain the EUV-CD spectra. This CD system, the development of which took five years, can be used to observe even weak natural CD spectra. The polarization characteristics of this system were also evaluated in order to calibrate the recorded CD spectra.

Keywords: circular dichroism; polarizing undulator; extreme ultraviolet region; amino acids; thin film; vacuum ultraviolet region; polarization analysis.

1. Introduction

The wavelength coverage of natural circular dichroism (CD) spectra can be extended to the vacuum ultraviolet (VUV) and higher energy regions by using synchrotron radiation as a light source. A combination of synchrotron radiation and a photoelastic modulator has been applied successfully to measure VUV-CD spectra in an attempt to detect chirality and obtain the structural information of proteins and other chiral molecules (Kadhane *et al.*, 2008; Nesgaard *et al.*, 2008; Pulm *et al.*, 1998; Wallace & Janes, 2001). This technique has been adopted at several synchrotron radiation facilities worldwide for accurate protein secondary structure analysis, such as at beamlines CD12 at SRS (UK) (Clarke & Jones, 2004), UV1 at ASTRID (Denmark), U9b and U11 at NSLS (USA), 3m-NIM1-C at BESSY2 (Germany), BL-15 at HiSOR (Japan) (Ojima *et al.*, 2001), DISCO at SOLEIL (France) (Miron *et al.*, 2005), 4B8 at BSRF (China), and CD1 at ISA (Denmark) (Miles *et al.*, 2007).

The extension of the CD-measurable region to the VUV and extreme ultraviolet (EUV; wavelengths shorter than 105 nm) regions has resulted in two valuable contributions to CD spectroscopy. The first contribution is the significant increase in the number of CD-applicable molecules. Since the electronic transition corresponding to the σ electron occurs in the VUV and EUV regions, the molecules devoid of chromophores, such as saturated carbon hydrides and alcohols, can be examined by CD spectroscopy in these regions. The other contribution is the significant increase in the information related to the structure of chiral molecules.

However, no natural CD of optical absorption in the EUV region has been reported, except for the magnetic CD (Koide *et al.*, 1991*a*) and CD in photoelectron spectroscopy (Nahon *et al.*, 2006), because the short-wavelength limit of CD spectra is restricted by the absorption edge of transmission-type optical elements. Typical materials used for fabricating optical elements that can be used in the VUV region are LiF and MgF_2 crystals, which can transmit in the VUV region at wavelengths longer than 105 and 115 nm, respectively, in principle. For example, a pioneering study on the VUV-CD spectroscopy of an amino acid (leucine) film has limited the wavelength region down to 135 nm (Meierhenrich *et al.*, 2005). Optical elements that can be used in the short-wavelength region, *i.e.* the EUV region, have not been developed thus far.

Recently, a CD measurement system without transmission-type optical elements has been developed at the BL-5B beamline at TERAS, Japan (Tanaka *et al.*, 2006; Yagi-Watanabe *et al.*, 2005*a*, 2007; Yamada *et al.*, 2005). This system consists of a polarizing undulator, which is used as an insertion device for synchrotron radiation and emits polarized light. Since this undulator (Onuki, 1986; Yagi & Onuki, 1996) can produce polarized light by AC modulation, it is the most

suitable light source for CD spectroscopy in the EUV region. An electromagnetic crossed overlapped undulator used at beamline SU5 at Super-ACO, which is based on the Onuki-type undulator, produces radiation in various polarization states in the VUV and EUV regions (Nahon & Alcaraz, 2004). This undulator can be used for obtaining spectra of CD in photoelectron spectroscopy (Nahon *et al.*, 2006) without AC modulation because of strong CD intensity (1–20% of the mean photoelectron intensity). In general, signals of natural CD of optical absorption are relatively weak (∼0.01–1% of absorption intensity); hence, AC modulation of circular polarization is essential. Natural CD spectra at wavelengths down to 130 nm have already been obtained with a sensitivity of approximately 0.01% by using our CD system (Kaneko *et al.*, 2009; Yagi-Watanabe *et al.*, 2007).

In this paper, the first observation of natural CD spectra in the EUV region by using the undulator-based CD system is reported. A thin alanine (Ala) film deposited on sodium salicylate (SS) coated glass is used as a sample. The obtained EUV-CD spectra are compared with those obtained by theoretical calculations. Prior to the CD measurement, the performance of the CD system in the EUV region is also evaluated by polarization analysis and intensity measurement under various experimental conditions.

2. Polarizing undulator and beamline BL-5B at TERAS

The beamline BL-5B has been dedicated to measuring the CD and linear dichroism (LD) spectra in the VUV and EUV regions (Tanaka *et al.*, 2006; Yagi-Watanabe *et al.*, 2005*a*, 2007; Yamada *et al.*, 2005). As a polarized light source, this beamline is equipped with a four-period Onuki-type undulator (Onuki, 1986; Yagi & Onuki, 1996). Fig. 1 shows a schematic view of this undulator, and Table 1 lists its specifications. The peak energy of undulator radiation can be selected by changing the electron energy E in the storage ring and the strength of the magnetic field, which is determined by the vertical distance between the magnets of the undulator (undulator gap).

The main advantage of this undulator is that the state of polarization of radiation can be modulated. By changing the relative phase retardation between the crossed magnetic fields of this undulator, radiation in left and right circular polarization states and vertical and horizontal linear polarization states can be produced. The polarization state of undulator

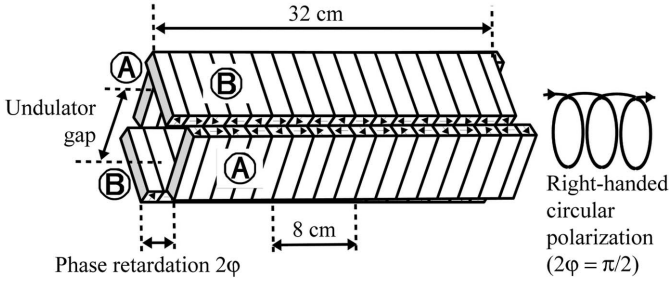

Figure 1
Schematic view of the Onuki-type undulator installed at TERAS.

Table 1
Specifications of the Onuki-type undulator installed at TERAS.

Overall length	320 mm
Magnet period	80 mm
Number of periods	4
Undulator gap distance	60–90 mm
Maximum magnetic field	0.15 T
Maximum K value	1.1
Typical modulation frequency	2 Hz

radiation can be modulated up to a modulation frequency f of 5 Hz. This frequency f is sufficient for the modulation spectroscopy, which is essential for obtaining spectra from weak CD signals. Additionally, the relatively wide bandwidth (∼30%) of the radiation emitted from this undulator is suitable for spectroscopy.

Such relatively high f values can be attributed to the compactness of the undulator. The overall length of this undulator is only 320 mm. In addition, this compact undulator can be easily installed in a small straight section of a storage ring.

A disadvantage of the undulator is that the radiation produced has a low intensity. Since the undulator gap in crossed-type undulators cannot be decreased beyond a certain limit, it is difficult to increase the intensity by increasing the strength of magnetic fields. However, the light intensity in the case of our system is sufficient for the CD measurement in optical absorption. Moreover, high intensity causes the photodecomposition of biomaterial samples and corresponding changes in their spectra. No changes are observed in the CD and absorption spectra during CD measurements performed for approximately 10 h using our system. Thus, the undulator is suitable for the CD measurement of biomaterial samples. Furthermore, this compact undulator can be used as an insertion device even in third-generation storage rings.

The beamline consists of a reflecting optical system comprising a prefocusing mirror and a grating, as shown in Fig. 2. The light emitted is deflected and focused by the prefocusing mirror, which is coated with Al, Au or Pt, with an angle of 15° between the incident light and reflected light. The light is monochromated by a Seya-Namioka-type monochromator with a 70.25° deviation angle, which is equipped with three interchangeable concave gratings [G1: 2400 grooves (gr) mm^{-1} with Al + MgF_2 coating; G2: 2400 gr mm^{-1} with Pt coating; and G3: 3600 gr mm^{-1} with Pt coating]. These simple optics have been designed in an attempt to minimize the degradation of polarization. Three four-blade slits are used to block the stray light. The intensity of stray light is estimated to be less than 1% in the EUV region by measuring the light intensity through a Pyrex glass window. Details of the beamline have been given in our previous report (Yagi-Watanabe *et al.*, 2007).

3. Polarization and intensity characteristics in the EUV region

The performance of the beamline is evaluated using several sets of E, lengths of undulator gap, gratings and mirrors. The

Table 2
Parameters for intensity, calibration factor and CD measurements.

Condition	E (MeV)†	Gap (mm)‡	Grating	Mirror
I	400	60	G1§	Al
II	400	60	G3¶	Au
III	500	60	G3¶	Au
IV	650	60	G3¶	Pt
V	650	65	G3¶	Pt

† Electron energy in the storage ring. ‡ Undulator gap distance. § 2400 gr mm^{-1} with Al + MgF_2 coating. ¶ 3600 gr mm^{-1} with Pt coating.

selected experimental conditions are listed in Table 2. The normalized intensity spectra of undulator radiation in the EUV and VUV regions under various experimental conditions are shown in Fig. 3(*a*). The intensity spectra have been normalized by the spectra obtained for the maximum undulator gap (90 mm) in order to eliminate the contribution of reflectances of optical elements. The undulator radiation centred at approximately 150 nm with the ∼30% bandwidth can be used under condition (II).

At TERAS, the users can easily select the value of E at each injection in the range 315 to 760 MeV. Hence, the first harmonic peak is shifted mainly by changing E instead of the undulator gap. This is because the light intensity rapidly decreases with an increase in undulator gap of our undulator. When E is increased to 500 and 650 MeV, the first harmonic peak shifts to 100 and 60 nm, respectively. This peak is also found to shift when the undulator gap is between 60 and 65 mm at E = 650 MeV. For wavelengths longer than 120 nm,

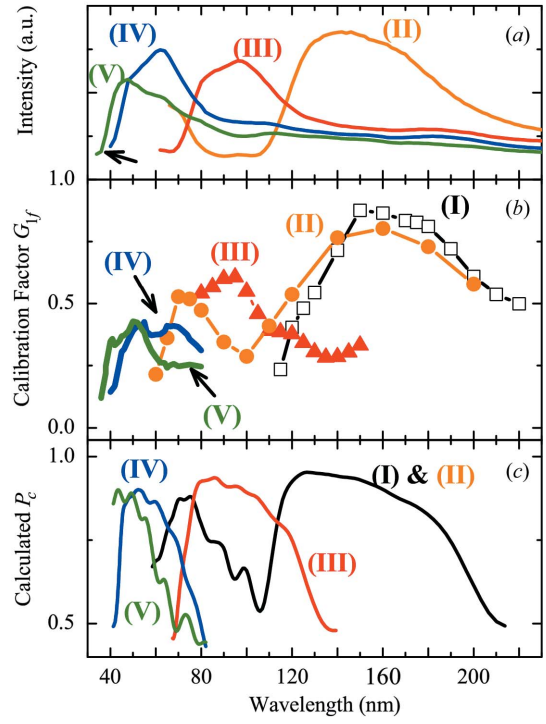

Figure 3
(*a*) Intensity spectra of light emitted from the undulator, (*b*) experimental values of the calibration factor G_{1f} expressed as a function of wavelength, and (*c*) calculated values of P_c from undulator radiation under several experimental conditions: condition (I) black lines; (II) orange lines; (III) red lines; (IV) blue lines; (V) green lines. Detailed parameters for each condition are summarized in Table 2.

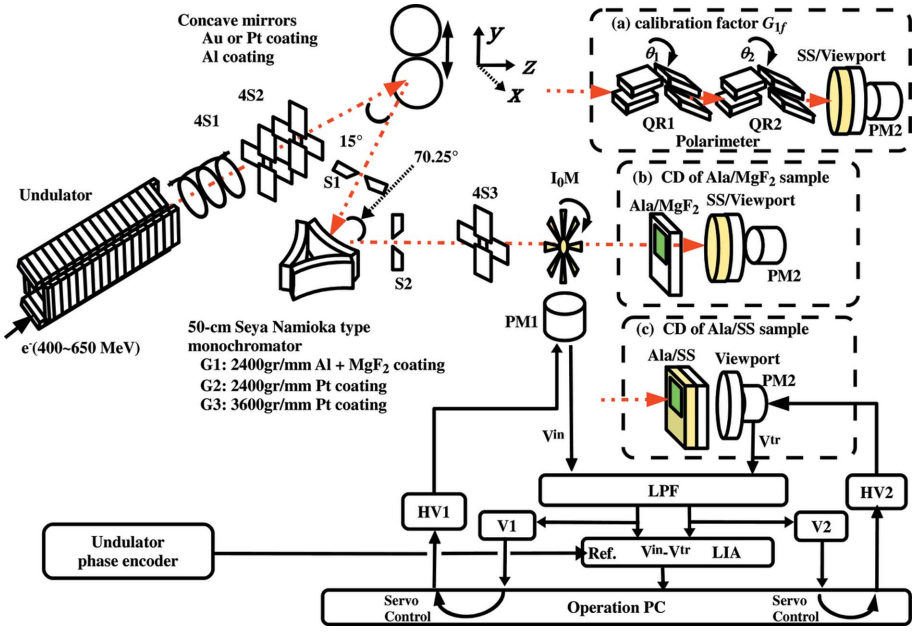

Figure 2
Schematic drawing of the optical arrangement of the TERAS BL-5B beamline and systems for measurements of (*a*) calibration factor G_{1f}, (*b*) CD spectra of Ala/MgF_2 sample, and (*c*) CD spectra of Ala/SS sample. 4S1–4S3: four-blade slits; S1 and S2: entrance and exit slits; I_0M: SS-coated chopper wheel which is used for monitoring the incident light intensity; PM1 and PM2: photomultipliers; HV1 and HV2: power supplies; LPF: electrical low-pass filter; V1 and V2: digital voltmeters; and LIA: dual-phase lock-in amplifier.

the CD experiment is usually performed under condition (I) rather than condition (II). This is because the reflectivity of Al and MgF_2-coated Al is several times larger than that of Au or Pt in this wavelength region. However, in the EUV region the reflectivity of Al becomes almost zero.

The assessment of polarization of the light incident on a sample is of considerable significance for the calibration of the CD spectra. In order to obtain accurate CD spectra, the polarization state of radiation emitted from the undulator has to be evaluated strictly because polarization depends on wavelength and the degradation of polarization can be attributed to the reflecting optical system. Recently, an accurate calibration method for AC modulation spectroscopy in the VUV region has been developed (Tanaka *et al.*, 2008*a*). This method introduces a calibration factor (G_{1f}) for calibrating the CD spectra recorded using our system with respect to real CD. The recorded CD signal is divided by the G_{1f} value. The

factor G_{1f} mainly depends on the value of circular polarization (P_c) emitted from the undulator and the polarization characteristics of the beamline. Indeed, this factor has been successfully used to calibrate the CD and LD spectra of standard samples with a mean difference of 7% from the standard in the wavelength region down to 185 nm (Tanaka *et al.*, 2008*a*). Moreover, the spectra obtained in this study exhibit a good agreement with the standard spectrum. In this study, the above-mentioned method is used to obtain spectra in the EUV region.

Next, we briefly explain the procedure for determining the G_{1f} value using a compact multiple-reflection-type polarimeter (Yagi-Watanabe *et al.*, 2005*b*). By using a similar type of polarimeter, the polarization states in the VUV and EUV regions are studied at several synchrotron radiation beamlines (Cubric *et al.*, 1999; Finetti *et al.*, 2004; Koide *et al.*, 1991*b*; Nahon & Alcaraz, 2004; Wang *et al.*, 2007). The polarimeter consists of a 1 mm-diameter aperture and two quadruple reflectors, QR1 and QR2, that function as phase shifters as well as quasi-linear polarizers. The polarization characteristics of the polarimeter are preliminarily determined by employing linearly polarized radiation. The intensity of the light transmitted through the polarimeter is recorded as a function of the rotation angle of QR1 and QR2, θ_1 and θ_2, respectively, in the *XY* plane, as shown in Fig. 2(*a*). Since the undulator modulates during the experiment with *f*, the recorded signal consists of a 1*f* component as well as a DC component. The signals of the 1*f* and DC components are detected using a lock-in amplifier (LIA) and a conventional voltmeter (V2), respectively, as in the case of CD measurement. The G_{1f} value can be determined from the θ_1 and θ_2 dependence of the 1*f* and DC components. In our experiment, θ_1 and θ_2 dependence is observed at every 45° and 20°, respectively. Details of this calibration method have been described in our recent paper (Tanaka *et al.*, 2008*a*). In addition, the values of P_c from the undulator using the *SPECTRA* program (Tanaka & Kitamura, 2001) and the parameters of the observed magnetic fields and the storage ring (Yagi *et al.*, 1995) have been computed.

Fig. 3(*b*) shows the obtained G_{1f} spectra in the EUV and VUV regions under various experimental conditions. The wavelengths corresponding to the peaks are almost analogous to those of the intensity spectrum. Under condition (II), the peak of G_{1f} corresponding to the second harmonic radiation is observed at a wavelength around 70 nm. The average experimental error in the G_{1f} values is estimated to be ±3%. The G_{1f} values moderately vary as a function of wavelength, especially at the long wavelength tail, as compared with the rapid decrease in intensity spectra.

The relatively small variation in the G_{1f} values show that CD signals can be detected even at the tail of undulator radiation. Hence, a relatively wide scanning range for recording CD spectra can be obtained without changing the undulator gap. From Fig. 3(*b*), it is found that under conditions (I) and (II) the first harmonic radiation covers wavelengths in the range 120 to 200 nm in which the conventional optical elements made of materials such as MgF_2 can be used.

From these results it is found that the CD measurement range can be extended to wavelengths down to 50 nm by tuning *E* to 500 and 650 MeV. Additionally, widening the undulator gap to 65 mm at *E* = 650 MeV results in the blue shift of the G_{1f} spectra, for which the CD measurement range can be extended to wavelengths down to 40 nm. This result indicates that our system can be used for the measurement of CD spectra in the VUV and EUV regions.

It is observed that the maximum G_{1f} values decrease with the wavelength, especially in the EUV region. The decrease in G_{1f} directly leads to the reduction in the intensity of the recorded CD signals. The maximum G_{1f} value under condition (IV) is approximately half that under condition (I). On the other hand, the maximum values of the calculated P_c are clearly independent of the wavelength, as shown in Fig. 3(*c*).

The decrease in G_{1f} in the EUV region is mainly due to the polarization characteristics of optics, probably the grating. The incident angle of 35° at the Seya-Namioka-type monochromator is expected to induce a significant difference in the reflectivity and phase of the *s*- and *p*-polarization components of undulator radiation. For example, the clear dip at 50 nm observed in the G_{1f} spectrum under condition (IV) is considered to have originated from the characteristic reflectivity of Pt (Hunter *et al.*, 1979).

It was also found that the G_{1f} value under condition (I) dropped faster than that under condition (II) in the short-wavelength region. This discrepancy was attributed to the difference in the coating material of optics. In addition, the ratio of G_{1f} of the first and the second harmonic radiations under condition (II) was approximately 0.66, whereas that of the calculated P_c values was approximate 0.93. These results strongly indicated that the wavelength dispersion of the polarization characteristics of optics also affected the G_{1f} values significantly. Since the effect of the polarization characteristics of optics is a disadvantage in our optical system, the G_{1f} values under each experimental condition were carefully determined for obtaining accurate CD spectra.

4. Experimental procedure for EUV-CD measurement

In spite of the above-mentioned disadvantage, EUV-CD spectra were recorded in the wavelength region down to 80 nm by the AC modulation of the undulator. L- and D-Ala thin films deposited on SS (Ala/SS) and MgF_2 (Ala/MgF_2) substrates were used as samples. Since substrates are normally opaque in the EUV region, Ala films were directly fabricated on an SS layer, which was commonly used in scintillators. SS was sprayed on a glass substrate. Ala films were deposited on both substrates by the vacuum sublimation technique, and the film thickness was monitored by using a quartz oscillator. Several Ala/SS samples with various thicknesses (20–30 nm) were prepared. The Ala powders were purchased from Wako Chemical and used without further purification. A detailed description of film preparation has been reported elsewhere (Tanaka *et al.*, 2002).

The CD spectra in the VUV and EUV regions have also been measured at BL-5B at TERAS. Next, the procedure of

CD measurement using the undulator-modulated technique is explained briefly. The value of f of our Onuki-type crossed undulator was set at 2 Hz. The CD spectra of Ala/MgF_2 and Ala/SS were recorded under conditions (I) and (III), respectively. The optical layout of the CD measurement for each sample is schematically shown in Figs. 2(*b*) and 2(*c*). The intensities of both the light incident on the samples (V^{in}) and that transmitted through the samples (V^{tr}) were detected using photomultipliers (PM1 and PM2). An SS-coated chopper wheel was used for monitoring the incident light intensity (I_0M). It chopped the light at a frequency of approximately 120 Hz. Such a chopper wheel has been used in a previous study for monitoring incident light in order to obtain a relatively flat baseline in CD spectra (Yagi-Watanabe *et al.*, 2007). The light passing through the Ala/MgF_2 sample was converted to visible light by the SS coating inside a glass viewport (SS/Viewport) and detected by PM2. In the case of Ala/SS, the light passing through the Ala film was immediately converted to visible light by the SS coating on the glass substrate and detected by PM2 through a bare glass viewport.

The output signals, V^{in} and V^{tr}, were fed to an electrical low-pass filter (LPF) with a cut-off frequency of 10 Hz for filtering the AC signal with the chopping frequency. Hence, both signals consisted of DC, 1f (2 Hz) and 2f (4 Hz) components and noise. The AC signals of the 1f and 2f components mainly corresponded to CD and LD signals, respectively. In this study the intensities of the DC signals for both outputs were maintained to be equal and constant by the servo control of the power supplies of PM1 and PM2 (HV1 and HV2, respectively) through the feedback from the DC components. The differential signal between the outputs ($V^{in} - V^{tr}$) was processed by LIAs while maintaining the DC signals to be the same; f was considered to be the reference frequency. Then, the AC signal picked up by an LIA operated in the 1f mode mainly contained the CD signal. In addition, an LIA operated in the 2f mode was used to detect the LD signal simultaneously. A detailed description of BL-5B and the procedure of CD observation have been given in our recent paper (Yagi-Watanabe *et al.*, 2007). The CD spectra of Ala/MgF_2 were also measured using a calibrated conventional CD spectrophotometer (J720WI, JASCO) in the wavelength range down to 185 nm. This spectrophotometer was calibrated using a standard CD sample of an aqueous solution of ammonium 10-camphorsulfonate (Takakuwa *et al.*, 1985).

CD and LD spectra were measured at several rotation angles of samples in order to evaluate the effect of linear anisotropy. If a sample has linear anisotropy, the recorded CD spectrum consists of a signal originating from linear anisotropy as well as a real CD signal (Tanaka *et al.*, 2006). Since CD and LD spectra were found to be independent of the rotation angles, the samples were assumed to be free from linear anisotropy. Fig. 4(*a*) shows an atomic force microscope (AFM) image of L-Ala film on SiO_2, whose film thickness was 50 nm. This result directly indicated that our Ala film was an aggregate of randomly orientated microcrystallites. Such a random orientation of microcrystallites cancelled out the effect of linear anisotropy.

We measured the CD spectra of the L- and D-Ala samples whose thicknesses are almost the same and subtracted the CD spectra of D-Ala film from those of L-Ala in order to compensate for the small apparent CD baseline in our CD system (Kaneko *et al.*, 2009). The real CD signal obtained by the above-mentioned procedure was calibrated by the determined G_{1f} value and normalized by the film thickness to calculate the circular dichroic coefficient $\Delta\mu$. It was confirmed that no spectral change in CD and absorption spectra was introduced by VUV and EUV irradiation during CD measurement.

A theoretical CD spectrum was calculated using the *Gaussian03* program package. The time-dependent density functional theory (TDDFT) method employing the B3LYP functional in combination with the 6-31 + $G(d,p)$ basis set was applied to calculate the rotational strength of an isolated L-Ala molecule in a zwitterionic state. The existence of the

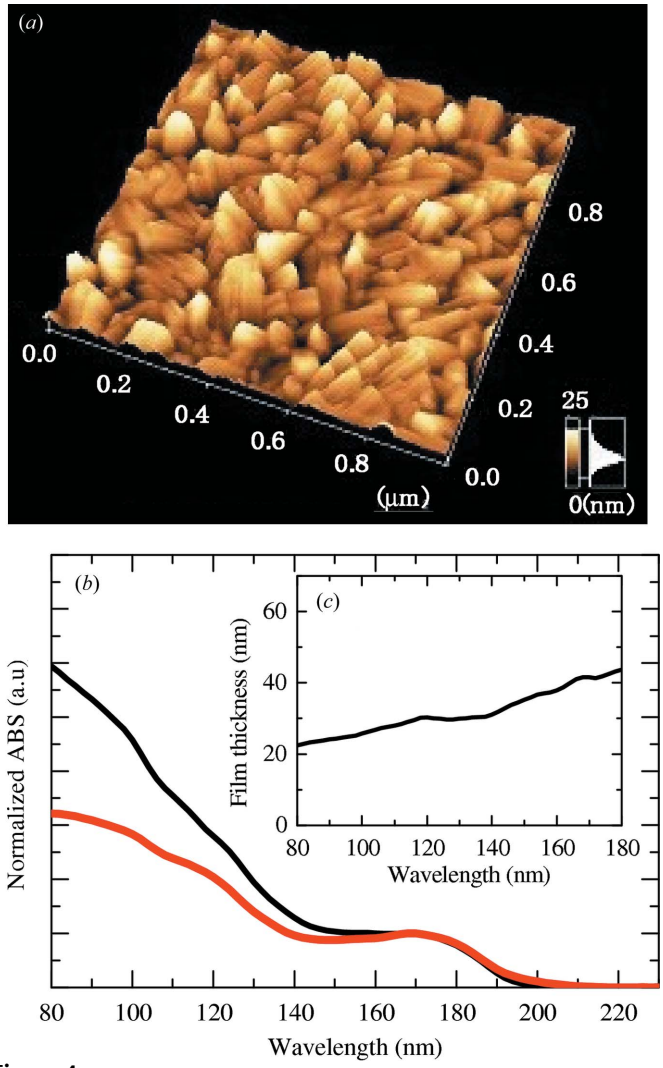

Figure 4
(*a*) AFM image of L-Ala film on SiO_2, whose film thickness was 50 nm. (*b*) Tentative normalized absorption spectrum of L-Ala/SS under condition (III) (red line) and reported spectrum of L-Ala (black line) (Kamohara *et al.*, 2008). (*c*) Effective thickness of L-Ala/SS calculated from reported absorption coefficient as a function of wavelength.

zwitterionic state in the solid phase was confirmed by single-crystal neutron diffraction (Wilson *et al.*, 2005) and X-ray photoelectron spectroscopy (Clark *et al.*, 1976). The molecular structure of L-Ala used in the CD calculation was obtained from the experimental data of neutron diffraction at 295 K (Wilson *et al.*, 2005). The theoretical CD spectrum was obtained by the convolution of Gaussian functions for each rotational strength, where the half-width of the Gaussian function at $1/e$ of the maximum was 0.33 eV (Kaneko *et al.*, 2009). The shortest excitation wavelength for calculating the rotational strength was approximately 65 nm. A detailed description of theoretical calculations has been reported elsewhere (Kaneko *et al.*, 2009).

5. Results and discussion

First, the suitability of the SS substrate for CD and absorption measurements is evaluated. An SS substrate with a flat surface such as MgF_2 crystal substrates cannot be prepared by spray technique. The surface roughness of the SS substrate has an undesirable effect on absorption measurement and the determination of film thickness. Fig. 4(*b*) shows a comparison of tentative absorption spectra of Ala/SS measured under condition (III) with reported spectra (Kamohara *et al.*, 2008), which are normalized by the intensities at a wavelength of 170 nm. A discrepancy is found between the absorption coefficients of the measured and reported spectra with an increase in the absorption coefficient. This discrepancy can be attributed to the surface roughness of the SS substrate. The effective thickness reduces with an increase in the absorption coefficient. Therefore, the effective thickness is approximately regarded to exhibit wavelength dispersion that can be determined by using the reported absorption coefficient, as shown in Fig. 4(*c*). The obtained CD spectra were also normalized by the wavelength dispersion of the effective thickness of each sample. The average effective thickness of each film is approximately 20–30 nm. Note that the macroscopical uniformity of film thickness is confirmed by the rotation angle dependence of the absorption spectra.

In order to evaluate the suitability of the Ala/SS sample for CD measurement the CD spectra of Ala/SS are compared with those of Ala/MgF_2. The spectra of L-Ala/SS are normalized by considering the wavelength dispersion of the effective thickness. In spite of the non-uniformity of thickness, the obtained CD spectrum of L-Ala/SS under condition (I) shows a good agreement with that of Ala/MgF_2 within the experimental error, as shown in Fig. 5. This result directly shows that the SS substrate is suitable for CD measurement. For measuring CD spectra in the short-wavelength region, in which the absorption coefficient is large, the development of scintillators in the EUV region with a flat surface such as inorganic crystals is being investigated.

The calibrated CD spectra and absorption spectrum of L-Ala films under each experimental condition are shown in Fig. 6(*a*). In the wavelength region down to 185 nm, the calibrated CD spectrum of Ala/MgF_2 under condition (I) shows a good agreement with that measured using the calibrated CD

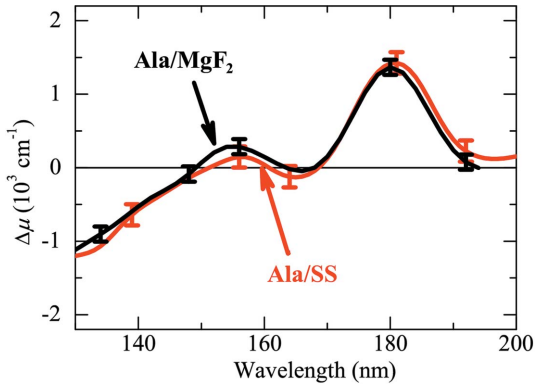

Figure 5
Comparison of calibrated CD spectra of L-Ala/SS (red line) and L-Ala/MgF_2 (black line) measured under condition (I).

spectrophotometer (Kaneko *et al.*, 2009). This result also strongly supports the accuracy of the determined G_{1f} values.

The calibrated EUV-CD spectrum down to a wavelength of 80 nm is shown in Fig. 6(*a*). This spectrum was obtained by averaging each CD spectrum of Ala/SS sample with the mean effective thickness of 20–30 nm. No significant change in these CD spectra was observed. It should be noted that a good agreement between these two CD spectra was found in the wavelength region from 130 to 150 nm within the experimental error. Typical values of the error were approximately 100 cm^{-1} in both spectra. This result indicated the suitability of the sample for EUV-CD measurement and the accuracy of the G_{1f} values.

The CD spectrum of the L-Ala film in the VUV and EUV regions shows a characteristic feature. A large negative peak

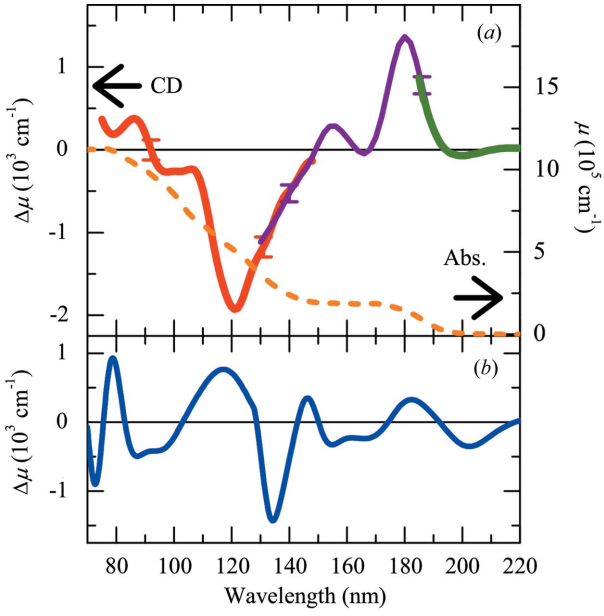

Figure 6
(*a*) Calibrated CD spectra of L-Ala/SS under condition (III) (red solid line) and of L-Ala/MgF_2 under condition (I) (purple solid line), spectrum measured using CD spectrophotometer (green solid line) (Kaneko *et al.*, 2009), and absorption spectrum of L-Ala (orange dashed line) (Kamohara *et al.*, 2008). (*b*) Calculated CD spectrum of the L-Ala isolated molecule in zwitterionic state.

at around 120 nm and a positive CD signal at wavelengths shorter than 90 nm are observed in the wavelength region shorter than 130 nm. However, the absorption spectrum exhibits only a gradual increase in this region. In addition, several CD peaks are also found in the VUV region (Kaneko *et al.*, 2009). The first CD peak with a low intensity and a negative sign exists around the absorption edge of 200 nm, which corresponds to the $n \rightarrow \pi^*$ transition of the COO^- group. The second and third CD peaks with positive signs are found at around 180 and 155 nm, which may be ascribed to the $\pi_0 \rightarrow \pi^*$ transition of the COO^- group and the $\pi_1(COO^-) \rightarrow \sigma^*(N-H)$ transition mixed with the $n \rightarrow \pi^*$ transition of the COO^- group, respectively (Kaneko *et al.*, 2009).

In the CD study of amino acids, no CD band in the short-wavelength region has been reported (Matsuo *et al.*, 2002; Meierhenrich *et al.*, 2005; Snyder *et al.*, 1973). The CD spectrum of L-Ala aqueous solution shows only two positive peaks at around 184 and 203 nm in the wavelength range down to 140 nm (Matsuo *et al.*, 2002). Moreover, the CD spectrum of the D-Leu thick film (thickness $\simeq$ 0.2–1 μm) deposited on MgF_2 also does not show the CD band in the wavelength range from 165 to 135 nm. This spectrum exhibits a negative peak, a positive peak and a positive shoulder at 207, 191 and 175 nm, respectively (Meierhenrich *et al.*, 2005). In these CD studies the wavelength limit of the photoelastic modulator and strong absorption of the solvent and thick film probably prevented the observation of CD spectra in the short-wavelength region. A detailed discussion on the variation in CD spectra of solids and solutions will be reported elsewhere.

The above-mentioned features have also been roughly predicted by our TDDFT calculations, as shown in Fig. 6(*b*). The calculated CD spectrum is blue-shifted by 0.6 eV in order to adjust the first negative and second positive CD peaks with respect to the experimental CD peaks at around 200 and 180 nm. The negative and positive peaks at approximately 160 and 145 nm in the calculated spectrum possibly correspond to the experimental CD dip and positive peak at approximately 165 nm and 155 nm, respectively. The experimental strong negative CD peak observed at around 120 nm has been successfully predicted at approximately 135 nm in the calculated spectrum, although some disagreement in peak wavelength has been found. The prediction of CD peaks in the short-wavelength region is inaccurate in the present stage. The two calculated positive CD peaks at around 117 and 80 nm may correspond to the experimental shoulder structure and positive peak at around 110 and 90 nm, respectively. Alternatively, the calculated peak at 117 nm may be ascribed to the experimental peak at 90 nm. The assignment of these CD peaks is difficult because various transitions overlap in the short-wavelength region. The contribution of the σ electron may increase with the photon energy. For more accurate prediction of CD spectra, a theoretical study based on more sophisticated calculations such as the symmetry adapted cluster (SAC) and SAC-configuration interaction method (Honda *et al.*, 2008) is necessary.

The asymmetric factor (so-called *g* factor) defined as the ratio of the CD coefficient to the absorption coefficient (CD/absorption) strongly contributed to the asymmetric photodecomposition induced by circularly polarized light. A pioneering study on the asymmetric photodecomposition of solid-phase amino acid induced by circularly polarized VUV has been reported by Meierhenrich *et al.* (2005). Unfortunately, the *g* factor in the solid state was not determined in this study. By using the obtained CD coefficients, the value of the *g* factor for the L-Ala film has been calculated to be +1.0% and −0.4% at ∼180 and 120 nm, respectively. It is difficult to determine the absorption coefficient at the absorption edge owing to the weak intensity and the effect of scattering. Despite this difficulty, the value of the *g* factor at 200 nm has been estimated to be approximately −2%, which is similar to that of the aqueous solution at around 200 nm (Nishino *et al.*, 2002). The value of the *g* factor tends to decrease in the short-wavelength region with an increase in absorption intensity.

Since the asymmetric photodecomposition of amino acid by circularly polarized light is a possible candidate for the origin of biomolecular homochirality (Bonner, 1995), our determination of the *g* factor in solid-phase amino acid provides important information. Our result indicates the less contribution of high-energy VUV light to biomolecular homochirality. However, the photodecomposition efficiency of the Ala film significantly increases with the photon energy in the VUV region; the quantum efficiencies of photodecomposition for around 200, 180 and 90 nm irradiation have been estimated to be 0.1, 0.2 and 1 (Tanaka *et al.*, 2008*b*). Hence, a detailed study on biomolecular homochirality focusing on photodecomposition efficiency and *g* factor has to be carried out.

Thus, we succeeded in observing the first natural CD observation in the EUV region down to 80 nm. The CD intensity of the negative peak at 120 nm was approximately 0.4% of the absorption intensity. Such a weak CD signal was acquired by an appreciable improvement in our undulator-based CD system over the past five years. The degradation of G_{1f} in the EUV region mainly caused by the deviation angle of the monochromator is the main disadvantage of the beamline. However, a careful evaluation of G_{1f} enabled us to obtain accurate CD spectra even in the EUV region. Since the Seya-Namioka-type monochromator has several practical advantages such as simple operation for changing output wavelength, the accurate evaluation of its polarization characteristics is important for carrying out polarization spectroscopy in the VUV and EUV regions. EUV-CD measurement in a short-wavelength region is being tested, and this study may provide important information on molecular structure. An accurate prediction of CD spectra will lead to conformational analysis of various chiral molecules and polymers in the future. Since most molecules exhibit strong absorption in the VUV and EUV regions, CD study in these regions may involve the conformational analysis of many chiral substances.

6. Conclusion

The natural CD-measurable region has been successfully extended to the EUV region down to a wavelength of 80 nm for the first time, by employing an undulator-based CD system

and an Ala/SS film. The suitability of SS substrates for CD measurement was evaluated by a comparison of the CD results with those of a conventional MgF_2 substrate. Our findings were also strongly supported by the reasonable agreement between the experimental and theoretical EUV-CD spectra. Prior to the EUV-CD measurement, the performance of our CD system was validated and the calibration factor was determined. In spite of the degradation of polarization in the short-wavelength region, this beamline could be used for CD measurement in the EUV region.

We would like to thank Dr H. Toyokawa for his technical assistance in the TERAS operation and the staff of the AIST Linac Group for their assistance in machine operation. A part of this study was financially supported by the Budget for Nuclear Research of the Ministry of Education, Sports, Science and Technology (MEXT), Japan, based on the screening and counselling by the Atomic Energy Commission. A part of this study was conducted at the AIST Nano-Processing Facility, supported by 'Nanotechnology Network Japan' of the MEXT, Japan.

References

Bonner, W. A. (1995). *Orig. Life Biosphere*, **25**, 175–190.
Clarke, D. T. & Jones, G. (2004). *J. Synchrotron Rad.* **11**, 142–149.
Clark, D. T., Peeling, J. & Colling, L. (1976). *Biochim. Biophys. Acta*, **453**, 533–545.
Cubric, D., Cooper, D. R., Lopes, M. C. A., Bolognesi, P. & King, G. C. (1999). *Meas. Sci. Technol.* **10**, 554–558.
Finetti, P., Holland, D. M. P., Latimer, C. J. & Binns, C. (2004). *Nucl. Instrum. Methods Phys. Res. B*, **215**, 565–576.
Honda, Y., Kurihara, A., Hada, M. & Nakatsuji, H. (2008). *J. Comput. Chem.* **29**, 612–621.
Hunter, W. R., Angel, D. W. & Hass, G. (1979). *J. Opt. Soc. Am.* **69**, 1695–1699.
Kadhane, U., Holm, A. I. S., Hoffmann, S. V. & Nielsen, S. B. (2008). *J. Photochem. Photobiol. A*, **197**, 110–114.
Kamohara, M., Izumi, Y., Tanaka, M., Okamoto, K., Tanaka, M., Kaneko, F., Kodama, Y., Koketsu, T. & Nakagawa, K. (2008). *Rad. Phys. Chem.* **77**, 1153–1155.
Kaneko, F., Yagi-Watanabe, K., Tanaka, M. & Nakagawa, K. (2009). *J. Phys. Soc. Jpn*, **78**, 013001.
Koide, T., Shidara, T., Fukutani, H., Yamaguchi, K., Fujimori, A. & Kimura, S. (1991*a*). *Phys. Rev. B*, **44**, 4697–4700.
Koide, T., Shidara, T., Yuri, M., Kandaka, N., Yamaguchi, K. & Fukutani, H. (1991*b*). *Nucl. Instrum. Methods Phys. Res. A*, **308**, 635–644.
Matsuo, K., Matsushima, Y., Fukuyama, T., Senba, S. & Gekko, K. (2002). *Chem. Lett.* **31**, 826–827.
Meierhenrich, U. J., Nahon, L., Alcaraz, C., Bredehöft, J. H., Hoffmann, S. V., Barbier, B. & Brack, A. (2005). *Angew. Chem. Int. Ed.* **44**, 5630–5634.
Miles, A. J., Hoffmann, S. V., Tao, Y., Janes, R. W. & Wallace, B. A. (2007). *Spectroscopy*, **21**, 245–255.
Miron, S., Refregier, M., Gilles, A. M. & Maurizot, J. C. (2005). *Biochim. Biophys. Acta*, **1724**, 425–431.
Nahon, L. & Alcaraz, C. (2004). *Appl. Opt.* **43**, 1024–1037.
Nahon, L., Garcia, G. A., Harding, C. J., Mikajlo, E. & Powis, I. (2006). *J. Chem. Phys.* **125**, 114309.
Nesgaard, L. W., Hoffmann, S. V., Andersen, C. B., Malmendal, A. & Otzen, D. E. (2008). *Biopolymers*, **89**, 779–795.
Nishino, H., Kosaka, A., Hembury, G. A., Matsushima, K. & Inoue, Y. (2002). *J. Chem. Soc. Perkin Trans. 2*, pp. 582–590.
Ojima, N., Sakai, K., Matsui, T., Fukazawa, T., Namatame, H., Taniguchi, M. & Gekko, K. (2001). *Chem. Lett.* **30**, 522–523.
Onuki, H. (1986). *Nucl. Instrum. Methods Phys. Res. A*, **246**, 94–98.
Pulm, F., Schramm, J., Lagier, H. & Hormes, J. (1998). *Enantiomer*, **3**, 315–322.
Snyder, P. A., Vipond, P. M. & Johnson Jr, W. C. (1973). *Biopolymers*, **12**, 975–992.
Takakuwa, T., Konno, T. & Meguro, H. (1985). *Anal. Sci.* **1**, 215–218.
Tanaka, M., Kaneko, F., Koketsu, T., Nakagawa, K. & Yamada, T. (2008*b*). *Radiat. Phys. Chem.* **77**, 1164–1168.
Tanaka, M., Kodama, Y. & Nakagawa, K. (2002). *Enantiomer*, **7**, 185–190.
Tanaka, M., Yagi-Watanabe, K., Kaneko, F. & Nakagawa, K. (2008*a*). *Rev. Sci. Instrum.* **79**, 083102.
Tanaka, M., Yagi-Watanabe, K., Yamada, T., Kaneko, F. & Nakagawa, K. (2006). *Chirality*, **18**, 196–204.
Tanaka, T. & Kitamura, H. (2001). *J. Synchrotron Rad.* **8**, 1221–1228.
Yagi, K. & Onuki, H. (1996). *J. Electron Spectrosc. Relat. Phenom.* **80**, 429–432.
Yagi, K., Yuri, M., Sugiyama, S. & Onuki, H. (1995). *Rev. Sci. Instrum.* **66**, 1993–1995.
Yagi-Watanabe, K., Tanaka, M., Kaneko, F. & Nakagawa, K. (2007). *Rev. Sci. Instrum.* **78**, 123106.
Yagi-Watanabe, K., Tanaka, M., Kaneko, F., Nakagawa, K. & Yuri, M. (2005*b*). *Nucl. Instrum. Methods Phys. Res. A*, **553**, 620–626.
Yagi-Watanabe, K., Yamada, T., Tanaka, M., Kaneko, F., Kitada, T., Ohta, Y. & Nakagawa, K. (2005*a*). *J. Electron Spectrosc. Relat. Phenom.* **144–147**, 1015–1018.
Yamada, T., Yagi-Watanabe, K., Tanaka, M., Kaneko, F., Kitada, T., Ohta, Y. & Nakagawa, K. (2005). *Rev. Sci. Instrum.* **76**, 093103.
Wallace, B. A. & Janes, R. W. (2001). *Curr. Opin. Chem. Biol.* **5**, 567–571.
Wang, Z. *et al.* (2007). *Appl. Phys. Lett.* **90**, 081910.
Wilson, C. C., Myles, D., Ghosi, M., Johnson, L. N. & Wang, W. (2005). *New J. Chem.* **29**, 1318–1322.